Journal of Physics: Conference Series

Substrate-removed flip-chip photodiode array based on *InAsSbP/InAs* double heterostructure

To cite this article: S A Karandashev *et al* 2019 *J. Phys.: Conf. Ser.* **1410** 012028

Substrate-removed flip-chip photodiode array based on *InAsSbP/InAs* double heterostructure

S A Karandashev[2,3], A A Klimov[1,2,3], R E Kunkov[1,3], A A Lavrov[2,3], T S Lukhmyrina[2], B A Matveev[2,3], M A Remennyi[2,3], A A Usikova[2,3]
[1]Peter the Great Saint-Petersburg Polytechnic University, Russia
[2]IR Optoelectronics Laboratory, Ioffe Institute RAS, St.Petersburg 194021, Russia
[3]IoffeLED Ltd., St. Petersburg 194064, Russia

Abstract. N-*InAsSbP/InAs/*P-*InAsSbP* double heterostructures have been grown onto n^+-InAs substrate and further processed into 2×2 photodiode array containing no n^+-*InAs*. C-V, spectral response as well as mid-IR photoluminescence and electroluminescence in the 77-300 K temperature range have been measured and used for photodiode characterization including D*(λ) and BLIP temperature evaluation.

1. Introduction

There is an increased demand for robust and efficient mid-IR (3-5 μm) LED-photodiode pairs that are useful for a number of analytical instruments [1]. *InAs* based detectors sensitive to wavelengths around 3.4 μm are still in the top list of extensive research efforts due to high performance parameters recently reported both for heterojunction unipolar [2] and homo p-n junction [3, 4] devices. The *InAsSbP/InAs* p-n heterostrutures are also good candidates for fabrication of mid-IR photodiodes (PDs) and multielement back-side illuminated (BSI) PD arrays as BLIP temperature as high as 180 K (2π FOV) [5] and room temperature Johnson noise limited operation at frequencies above 100-200 Hz [6] have been already demonstrated for single heterostructure (SH) PDs. Some recently obtained data suggests that *InAsSbP/InAs* double heterostructure (DH) PDs are superior to the SH ones in terms of the zero-bias resistance-area product R_0A - figure of merit of any diode. However, there have been no attempts to fabricate linear or 2D PD arrays based on *InAsSbP/InAs* DHs.

The paper presents first results on 2×2 PD array based on *InAsSbP/InAs* DH with broad spectral response, enhanced responsivity, individual addressing and suppressed optical and electrical cross talk between elements. These performance improvements have been achieved due to elimination of semi-transparent n^+-*InAs* substrate and implementation of flip-chip bonding method for the PD array fabrication.

2. Experimental details

Our DH samples initially contained 4 μm P-*InAsSbP(Zn)* (p~5×10^{17} cm^{-3}) wide gap contact layer, 6 μm n-*InAs* undoped absorbing active layer with donor concentration n= 5×10^{16} cm^{-3}, 2 μm N-*InAsSbP* undoped wide gap cladding layer, and finally a 350 μm heavily doped n^+-*InAs* (100) substrate (n^+ ~10^{18} cm^{-3}) semitransparentin the spectral range of interest (see fig.1). It follows from fig.1 that PDs with radiation transmitted through n^+-*InAs* substrate (back-side illumination mode – BSI) suffer from sufficient absorption at important for gas analysis wavelength of 3.4 μm. According to transmission data presented in fig.1 and in [7] electron concentration n^+ in our substrates is in the (2-3)×10^{18} cm^{-3} range.

The photoluminescence (PL) spectrum measured at 77 K in a reflection mode showed strong longwave emission peak around 0.4 eV which is a common value for the undoped n^{o}-*InAs*; PL spectrum contains also weak shortwave peak at 0.49 eV obviously related to recombination in P-*InAsSbP* (see fig. 2 (a)). Close to the above spectrum was recorded from reference N-*InAsSbP*/n^{+}-*InAs* sample also shown in fig.2 (a). Room temperature (RT) PL spectrum contain only single band corresponding to recombination in n-*InAs* active layer. Electroluminescence (EL) peaks matched the corresponding PL peaks at 77 K (hν = 0.4 eV) and 300 K (hν = 0.36 eV) (see fig 2 (b)). The RT EL peak value was typical for LEDs with n^{o}-*InAs* active layer, while the spectral shape contains Fabry-Perot fringes typical for thin LEDs with reflective anode and mirror out coupling surface [8].

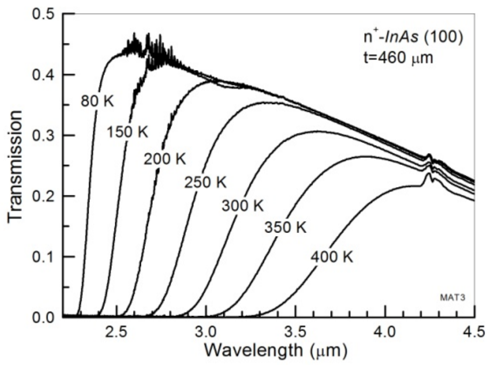

Figure 1. Transmission spectra of n^{+}-*InAs* substrate in the 80-400 K temperature range.

(a) (b)

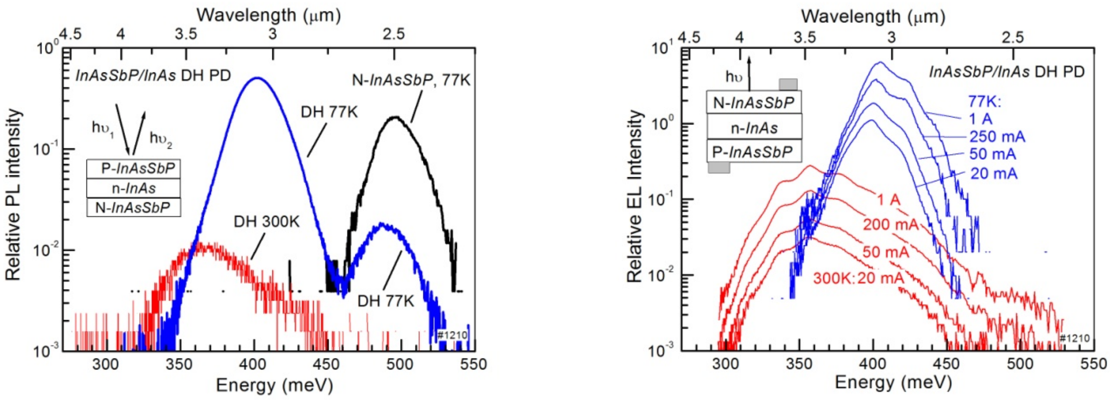

Figure 2. ‘‘Reflection” photo- (a) and electroluminescence (b) spectra in *InAsSbP/InAs* DH PD at 77 and 300 K.

Epitaxial wafers were subjected to standard multistage photolithography and wet chemical etching, which resulted in the formation of rectangular chip with a total size of ~1000×1000 μm (see fig. 3 (a)). The chip contained 4 photodiodes of 500×500 μm size each separated by ~20 μm deep grooves. Each photodiode had "cornertriangle" metal cathode denoted as "C" in fig.3(a) and broad metal anode denoted as "A"; the latter covered most of the 500×500 μm^{2} element area. Both anode and cathode were formed during evaporation of *Cr*, *Ni* and *Au* at vacuum with further "enhancement" by electrochemical deposition of *Au* with final thickness of about 2μm. The chip was mounted onto ceramic read-out board as shown in fig.3 (b). Prior measurements the ceramic submount surface was protected by a photoresist and n^{+}-*InAs* substrate shown by dashed rectangular in fig.3 (b) was

Journal of Physics: Conference Series **1410** (2019) 012028 doi:10.1088/1742-6596/1410/1/012028

completely removed by mechanical polishing and further chemical etching. The groove depth exceeded the total *InAsSbP/InAs/InAsSbP* DH thickness and because of this the above process resulted in getting 4 individual PDs mounted close to each other on a single submount without any electrical and mechanical interconnection and thus with negligible cross-talk between elements (see fig.3(c)). Contact pads in fig.3 are denoted as Ai and Ci for each of the 4 PD elements (i=1, 2, 3, 4).

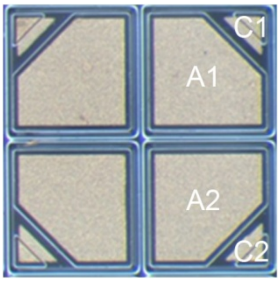

Figure 3 (a). Photo of the chip contact side.

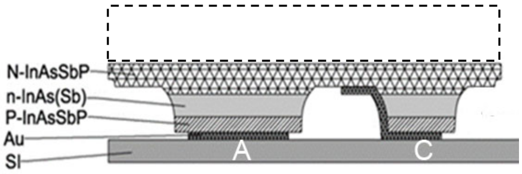

Figure 3 (b). Schematic of the diagonal cross section of the individual PD element mounted onto submount. Dashed rectangle – location of the n^+-*InAs* substrate prior removal.

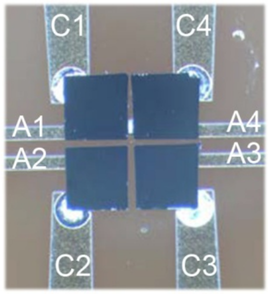

Figure 3 (c). Photo of the chip onto ceramic submount with anode and cathode bonding pads. View from the N-*InAsSbP* side.

Capacitance-voltage (C-V) characteristics exhibited linear dependence in the C^{-3}-V coordinates (see fig.4) indicating linear impurity distribution in the space charge region similar to the *InAsSbP/InAs* SH and DH described previously [5, 11]. However, the zero bias unit area values C_0/A are at least 2-fold smaller than the lowest values published for the *InAs* DH PDs in [11]. This makes good basis to creation in future high speed *InAs* matrix PDs.

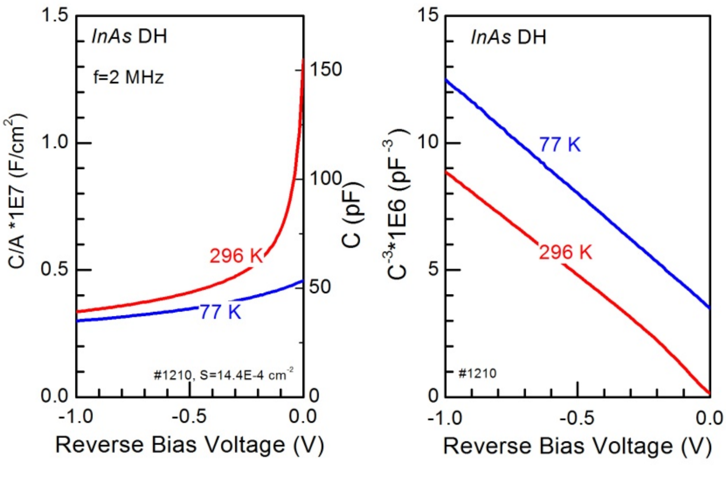

Figure 4. C-V characteristics at 77 and 296 K.

3. Results and discussion

At T>220 K the zero bias resistance $R_o$of the individual PDs exhibited temperature dependence that is typical for diodes with domination of the diffusion current as the activation energy of the exponential growth (R_o~exp(E_a/kT)) is close to that of the energy gap value (E_a= E_g = 0.41 eV (see fig. 5)). At low temperatures (T<220 K) the activation energy is roughly a half of the E_g indicating domination of the generation-recombination or tunnel current.

Spectral response near 2.7 μm was partly distorted by presence of water vapour and carbon dioxide in an optical path while the peak wavelength region contained Fabry-Perot fringes corresponding to the total DH thickness of L=11 μm and refractive index n=3.42: $\Delta\lambda=\lambda^2/2nL$ (see fig.6 with $\Delta\lambda_{mean}$=0.15 μm and also fig.2 (b) with fringes in the EL spectra). No fringes associated with reflection from semiconductor/air interface and anode contact have been observed at the shortwave shoulder of the spectral response because of high absorption in P-*InAsSbP* and in n-*InAs* layers. The responsivity slope at the shortwave shoulder at λ>2.6 μm and at T<360 K matches that of the ideal photodetector revealing independence of collection efficiency on wavelength. Thus we can conclude that the diffusion length of holes generated by radiation in N-*InAsSbP* is much larger than 2 μm - the thickness of the N-*InAsSbP* layer. The reason for the spectral response degradation at λ<2.6 μm and T<200 K (see the step at λ=2.6 μm) is not clear at the moment. At the same time the longwave shoulder exhibits no uncommon features, e.g. the temperature variation of the red cut-off wavelengths ($\lambda_{0.1}$ and $\lambda_{0.5}$ respectively) matches well with the known variation of *InAs* energy gap (see fig. 7): E_g= 415 - $0.28\times T^2/(T+83)$ [9, 10].

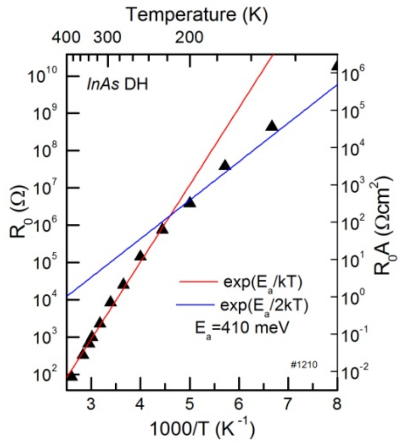

Figure 5. Zero bias resistance R_o vs temperature in single *InAsSbP/InAs* DH PD element.

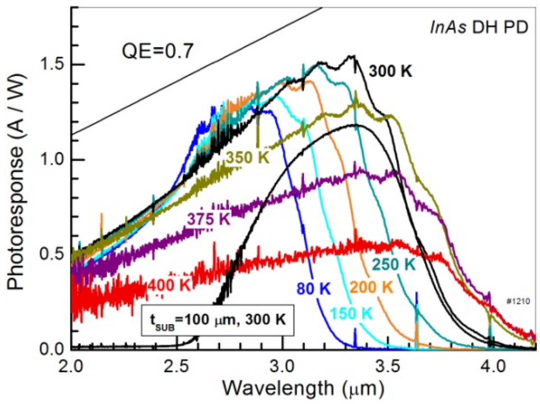

Figure 6. Spectral response of the individual PD element at several temperatures. Solid line presents responsivity of an ideal detector (QE=0.7). Narrow band response of the PD with t_{sub}=100 μm thick substrate is given for comparison.

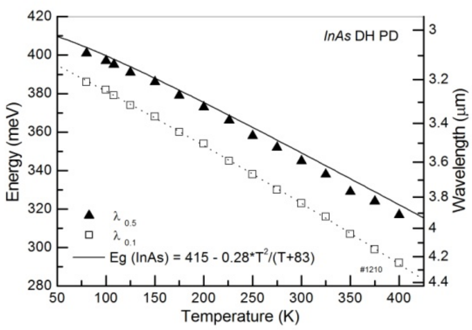

Figure 7. Red cut-off wavelength and energy vs temperature in *InAsSbP/InAs* DH PD.

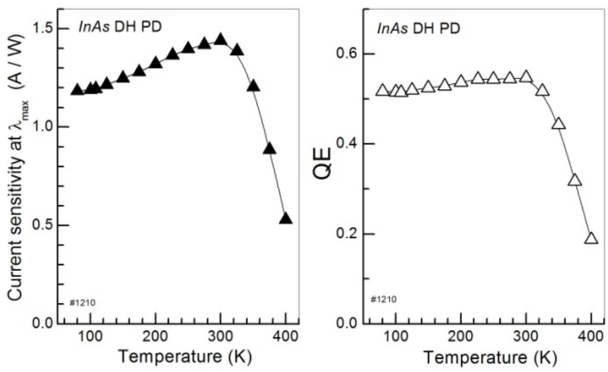

Figure 8. Current sensitivity and quantum efficiency at maximum vs temperature in *InAsSbP/InAs* DH PD.

Current sensitivity S_I and quantum efficiency at maximum in the DH PD free of substrate are shown in fig.8. Degradation of both S_I and QE at T>300 K are probably originate from N-*InAsSbP* layer transmission change.

Superposition of data presented in fig.5 and fig.6 enable us to simulate Johnson noise limited specific detectivity D* shown in fig.9. It follows from fig.9 that the D* value of the 2×2 array elements at room temperature is fairly close to the best values of the single element *InAsSbP/InAs* PDs known from literature and the BLIP operation mode is achieved at around 170 K for the 2π field of view which is close to data published for the *InAsSbP/InAs* SH PD [5]. However, spectral response of current array is much broader than that in [5] which may be essential in a curtain amount of applications.

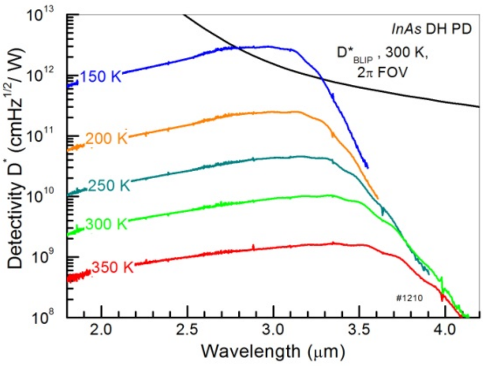

Figure 9. D* vs wavelength at several temperatures of the *InAsSbP/InAs* DH PD free of substrate.

Acknowledgments

We thank Il'inskaya N D for technical assistance in performing this research. The work performed at IoffeLED, Ltd. has been supported by the RF state program (ID: RFMEFI57618X0104).

References

[1] Matveev B A, Sotnikova G Yu, 2019 Optics and Spectroscopy, **127**, n.8 (in press)
[2] Savich G R, Pedrazzani J R, Sidor D E, Wicks G W 2013 Infrared Physics & Technology, **59,** 152 DOI: 10.1016/j.infrared.2012.12.031
[3] Sandall I C, ZhangSh, TanCh H 2013 OPTICS EXPRESS **21** 25780
[4] Maddox S J, Sun W, Lu Z, Nair H P, Campbell J C, Bank S R 2012 Appl. Phys.Lett., **101,** 151124
[5] Brunkov P N, Il'inskaya N D, Karandashev S A, Lavrov A A, Matveev B A, Remennyi M A,Stus' N M, Usikova A A, 2016 Infrared Physics & Technology, **78**, 249 http://dx.doi.org/10.1016/j.infrared.2016.08.013
[6] Dyakonova N, Karandashev S A, Levinshtein M E, Matveev B A, Remennyi M A, 2019 Semicond. Sci. Technol., **34,** 015013, DOI: 10.1088/1361-6641/aaf0c6
[7] Komkov O S, Firsov D D, Kovalishina E A, Petrov A S, 2014 PrikladnayaFizika, № 4 93 (in Russian).
[8] Zotova N V, Il'inskaya N D, Karandashev S A, Matveev B A,Remennyi M A, Stus' N M, 2008 Semiconductors, **42,** 625.
[9] Fang Z M, MaK Y, JawD H, Cohen, Stringfellow G B, 1990 J. Appl. Phys., **67,** 7034.
[10] http://www.matprop.ru/InAs_bandstr
[11] Brunkov P N, Il'inskaya N D, Karandashev S A, Lavrov A A, Matveev B A, Remennyi M A, Stus' N M, Usikova A A 2016 Infrared Physics & Technology. **76** 542. http://dx.doi.org/10.1016/j.infrared.2016.04.002